Electronic susceptibility of niobium*

J. F. Cooke, H. L. Davis, and Mark Mostoller
Solid State Division, Oak Ridge National Laboratory, Oak Ridge, Tennessee 37830
(Received 15 October 1973)

The static electronic susceptibility $\chi(\vec{q})$ is calculated for niobium along the [100] direction both with and without matrix elements. The energy bands are generated by a fitted second neighbor, *s-p-d* Slater-Koster model, and matrix elements are approximated by using the Slater-Koster wave-function coefficients with radial integrals of Fermi-level Korringa-Kohn-Rostoker wave functions within the muffin tin. The Brillouin-zone integration is carried out by the combined linear-quadratic method of Cooke and Wood. Contrary to the work of Evenson, Fleming, and Liu our constant-matrix-element calculation yields a result for $\chi(\vec{q})$, which is relatively featureless. The major effects of including the band and momentum dependence of the matrix elements are to make $\chi(\vec{q})$ a generally decreasing function of $|\vec{q}|$, and to bring out some structure not seen in the constant-matrix-element calculation. The static susceptibility has a noticeable hump around the same wave vector as the observed [100] LA-phonon anomaly. The frequency dependence of the real part of the dynamic susceptibility appears to be small for ω in the phonon-frequency range.

I. INTRODUCTION

The features of wave-vector- and frequency-dependent electronic susceptibilities are reflected by a wide variety of material properties. In the static magnetic susceptibility calculated for some rare earths, for example, peaks occur at characteristic wave vectors which correspond to the magnetic structures observed for these metals.[1] For the ferromagnetic transition metals, the sudden extinction of neutron-measured spin-wave peaks is related to a rapid change in the imaginary part of the magnetic susceptibility; the spin waves, which are collective modes of the system, decay quickly when they become degenerate with a high density of single-particle Stoner excitations.[2-4] In a number of high-T_c superconductors, including niobium, the observed phonon spectra contain anomalies which are not found in the spectra of neighboring materials with low transition temperatures.[5-8] Most of the explanations proposed for these anomalies rely on assumed special features of the electronic screening function, and thus are model oriented.[9-14] One means of testing the validity of these various explanations is to perform accurate susceptibility calculations.

Evenson, Fleming, and Liu[14] have calculated generalized static-susceptibility functions for several bcc transition metals by neglecting the momentum dependence of the matrix elements and using Mattheiss's tungsten band structure,[15] with the Fermi level adjusted to accommodate the proper number of electrons. Their results exhibited considerable structure, some of which they were able to correlate with observed properties such as the occurrence of anitferromagnetism in chromium, the helical magnetic structure of europium, and the LA-phonon anomaly along the [100] direction in niobium. They then speculated that some of the calculated structure which was uncorrelated with any observed property might be reduced in magnitude if the matrix elements were included. The more recent work of Gupta and Sinha[16] has an interesting bearing on this speculation. They calculated the static susceptibility of chromium, both with and without matrix elements, and their results do show the difference that matrix elements can make. However, they found that the inclusion of matrix elements reduced the susceptibility peak usually correlated with the occurrence of a spin-density wave in chromium.

In this paper, we report the results of susceptibility calculations for niobium along the [100] direction both with and without matrix elements. Instead of reducing structure, as was suggested by Evenson *et al.*[14] for niobium and found by Gupta and Sinha[16] for chromium, we find that including the band and momentum dependence of the matrix elements actually brings out structure not seen in the constant-matrix-element calculation. Our calculations are based on a realistic band structure, and are performed at two integration meshes to point out the need for computational accuracy. Section II describes our methods, results are presented in Sec. III, and Sec. IV briefly summarizes our present conclusions.

II. METHODS

In the random-phase approximation, the wave-vector- and frequency-dependent electron screening function is[17,18]

$$\epsilon(\vec{q}, \omega) = 1 + (8\pi e^2/q^2)\,\chi(\vec{q}, \omega), \tag{1}$$

$$\chi(\vec{q}, \omega) = \chi'(\vec{q}, \omega) + i\chi''(\vec{q}, \omega)$$

$$= \frac{1}{N} \sum_{\vec{k}} \sum_{n,n'} |(n', \vec{k}+\vec{q} \,|\, n, \vec{k})|^2 \times \frac{f(n,\vec{k}) - f(n', \vec{k}+\vec{q})}{E(n', \vec{k}+\vec{q}) - E(n,\vec{k}) - \hbar\omega - i\delta}, \quad (2)$$

where $E(n, \vec{k})$ is the electron energy in the band n at the wave vector $\vec{k}$, and $f(n, \vec{k})$ is the Fermi occupation factor. The static susceptibility is

$$\chi(\vec{q}) = \chi'(\vec{q}, 0) = \chi(\vec{q}, 0). \quad (3)$$

In terms of the Bloch eigenstates $\phi(n, \vec{k})$, the matrix elements are given by

$$(n', \vec{k}+\vec{q} \,|\, n, \vec{k}) = \int d^3r \, \phi^*(n', \vec{k}+\vec{q}) \, e^{i\vec{q}\cdot\vec{r}} \phi(n, \vec{k}). \quad (4)$$

The sum over $\vec{k}$ in Eq. (2) ranges over the first Brillouin zone (BZ), and if $\vec{k}+\vec{q}$ lies outside the first zone, it is translated back in by addition of the appropriate reciprocal-lattice vector. To calculate the susceptibility $\chi(\vec{q}, \omega)$ from Eq. (2), all that is required is a band structure, matrix elements, and an integration procedure.

To incorporate flexibility and minimize computational time, we use a second-neighbor, s-p-d Slater-Koster[19] interpolation scheme to generate the energy bands. The 27 parameters of the Slater-Koster model are determined from a least-squares fit to the results of first-principles band-structure calculations. As found by Connally,[20] the Slater-Koster model gives fits comparable to those expected from other interpolation schemes; for the bcc transition metals he found that the rms deviation for about 80 to 100 energies at various symmetry points is typically 0.001–0.004 Ry.

Consistent with our use of the Slater-Koster interpolation scheme for the energy bands, we approximate the matrix elements by a tight-binding approach. The matrix elements of Eq. (4) are first expressed in terms of orthogonalized Landshoff-Löwdin orbitals,[19] and all but the site-diagonal integrals are neglected. An expansion of $e^{i\vec{q}\cdot\vec{r}}$ in spherical harmonics gives

$$(n', \vec{k}+\vec{q} \,|\, n, \vec{k}) = 4\pi \sum_{lm, l'm'; LM} i^{-L} C^{LM}_{l'm', lm} \times a^*_{l'm'}(n', \vec{k}+\vec{q}) a_{lm}(n, \vec{k}) \times A(l', l, L; |\vec{q}|) Y_{LM}(\hat{q}), \quad (5)$$

where $a_{lm}(n, \vec{k})$ is the (Slater-Koster) expansion coefficient for the l, m angular-momentum component of the state $n, \vec{k}$ and $Y_{LM}(\hat{q})$ is the L, M spherical harmonic for the direction $\hat{q}$. For real spherical harmonics, the $C^{LM}_{l'm', lm}$ are Gaunt factors, which are obtainable from products of Clebsch-Gordan coefficients. The radial integrals in Eq. (5) are

$$A(l', l, L; |\vec{q}|) = \int_0^\infty dr r^2 R^*_{l'}(r) R_l(r) j_L(|\vec{q}| r), \quad (6)$$

in which $R_l(r)$ is the radial wave function, and $j_L(|\vec{q}| r)$ is the Lth spherical Bessel function.

We evaluate the radial integrals numerically using the wave functions of the Korringa-Kohn-Rostoker (KKR) calculations to which the Slater-Koster model is fitted: the integration is carried out over the muffin tin for the wave functions at the Fermi level. For the d functions, this should be a good approximation, since about 80% of the d-electron charge density lies within the muffin tin. For the s and p function, the approximation is not as good, but the character of the bands at and around the Fermi surface in niobium is predominantly d.

Given energy bands and matrix elements, the integral over the BZ in Eq. (2) must be done accurately. The procedure we use is the combined linear-quadratic method of Cooke and Wood.[21] The sum over the full zone is mapped onto a sum over an irreducible Brillouin zone (IBZ), which has $\frac{1}{48}$ of the volume of the full BZ. The IBZ is subdivided into cubes which are small enough so that the electronic energies can be expanded linearly in $\vec{k}$. The Fermi factor $f(n, \vec{k}) - f(n', \vec{k}+\vec{q})$ is taken to have magnitude zero or one depending on its value at the center of each small cube. We also assume that the matrix element does not change significantly over the volume of the small cube from its value at the center. As a result of these approximations the integration in each small cube can be performed analytically,[22] with the result depending on $a_{lm}(n, \vec{k}_c)$, $E(n, \vec{k}_c)$, and $\nabla_k E(n, \vec{k}_c)$, where $\vec{k}_c$ locates the center of a small cube. The total integral is then obtained by summing up the contributions from each of the small cubes.

The information needed to evaluate the BZ sum is obtained in the following manner. The Slater-Koster model is used to evaluate the electronic energies on a regular mesh of 506 points in the IBZ. The energies are then interpolated quadratically[23] to provide analytic expressions for $E(n, \vec{k})$ through the IBZ. The gradient of $E(n, \vec{k})$ is determined by differentiating these analytic expressions. Because of the difficulties arising from near degeneracies and band crossings, the $a_{lm}(n, \vec{k})$ are not interpolated, but are instead calculated directly from the Slater-Koster model at each $\vec{k}_c$.

Within this framework two different procedures were used to calculate $\chi(\vec{q})$. The real part of $\chi(\vec{q}, \omega = 0)$ can be calculated directly from Eq. (2) as a principle-value integral, or indirectly by first finding $\chi''(\vec{q}, \omega)$ and then performing a Hilbert or Kramers-Kronig transform to obtain the real part. The direct calculation has two advantages over the indirect procedure. First, the direct scheme is faster since it takes about 4.5 min per $\vec{q}$ point on the IBM model 360-91 as compared to about 6 min per $\vec{q}$ point for the indirect scheme when 3080 small cubes are used in the IBZ. Second, the indirect scheme generates a histogram

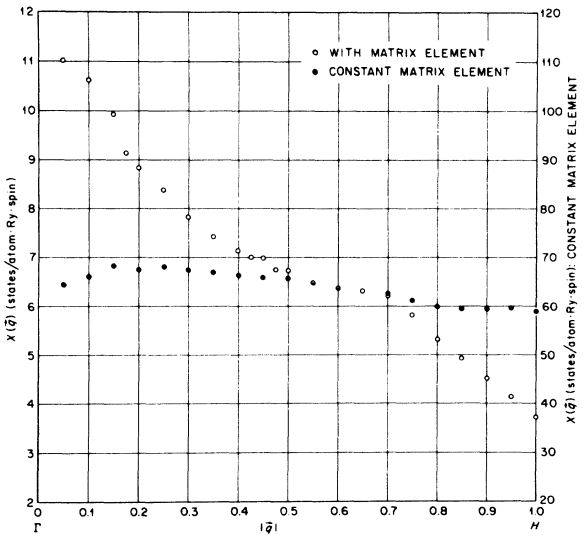

FIG. 1. Static susceptibility for niobium with $\vec{q}$ along [100] and $|\vec{q}|$ in reduced units of $2\pi/a$. Each point was calculated using 3080 cubes in the IBZ.

representation for the imaginary part of $\chi(\vec{q},\omega)$, which means that the real part can not be evaluated at $\omega = 0$, so that some sort of extrapolation must be performed to obtain $\chi(\vec{q})$. On the other hand, information about the full frequency dependence of χ'' and χ' can be obtained more efficiently by using the indirect method.

When a mesh of 3080 cubes is used in the IBZ, numerical results for $\chi(\vec{q})$ based on these two schemes agree typically to within 2%, with the indirect values being consistently higher than the direct values. The general features and important details of the results are, however, essentially the same. On the basis of these types of comparisons we feel that the numerical errors in our 3080-cube calculation are on the order of a few percent. Because of the advantages referred to above we have chosen to base the calculations of $\chi(\vec{q})$ presented in this paper on the direct scheme.

III. RESULTS

For the results presented here the parameters of the Slater-Koster interpolation scheme are fitted to KKR[24,25] energy bands generated from the muffin-tin potential of Deegan and Twose.[26] For 546 energies in the first six bands, the rms deviation of the Slater-Koster model from the KRR results is 0.0067 Ry.[27] This smooth Slater-Koster band structure is in good agreement with the results of Deegan and Twose (and of Mattheiss[28]) for the energy bands along symmetry directions, the Fermi surface, and the density of states.

The matrix elements, when included in the susceptibility, are calculated as previously described. In this approximation, the dominant effects are provided by the Gaunt factors, that is, by the combinational properties of the spherical harmonics rather than the details of the radial wave functions. In Eq. (5), the $l = l'$, $L = 0$ terms generally make the largest contributions because of the Gaunt factors. The corresponding radial integrals are largest for $\vec{q} = 0$, while the off-diagonal in l and l' terms have their maxima at nonzero $\vec{q}$ values.

Figure 1 shows the results for $\chi(\vec{q})$ along the [100] direction obtained by direct integration over a mesh of 3080 cubes in the IBZ. Figure 2 compares results determined by integration over a much coarser integration mesh of 440 cubes in the IBZ with those calculated on the fine mesh of 3080 cubes. The coarse mesh results exhibit scatter large enough to make it difficult to distinguish real from spurious structure in the curves. However, this scatter is not as large as that found by Evenson *et al.*, primarily because the analytic integration scheme is used in the small cubes instead of a trapezoidal rule.

Both with and without matrix elements, the susceptibility in Fig. 1 is relatively smoothly varying. The structure appearing in the calculation with momentum-dependent matrix elements is due primarily to the fact that Gaunt factors act as do selection rules which weight transitions between bands of the same wave-function character much more heavily than those connecting states of different characters. This also has the effect of reducing $\chi(\vec{q})$ by roughly an order of magnitude so

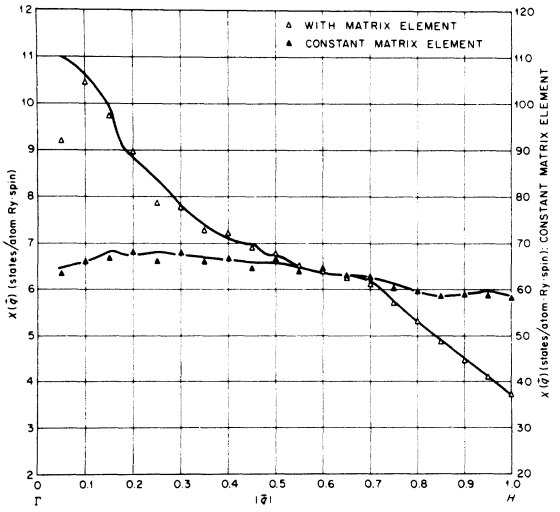

FIG. 2. Static susceptibility for niobium with $\vec{q}$ along [100] and $|\vec{q}|$ in reduced units of $2\pi/a$. The solid lines represent smooth curves through the points shown in Fig. 1 which were calculated using 3080 cubes in the IBZ. The triangles are results obtained using 440 cubes in the IBZ.

that it has the correct long-wavelength limit. The decrease in $\chi(\vec{q})$ with increasing $\vec{q}$ when the matrix elements are included is also consistent with the dominant role played by the $L=0$ contributions in Eq. (5). This effect is similar to what one finds for a form factor.

Besides the shoulder at $|\vec{q}| = 0.15$ and the smaller structure at $|\vec{q}| = 0.45$ and $|\vec{q}| = 0.50$ (which is around the limits of our computational accuracy, but may be associated with transitions across flat portions of the Fermi surface close to Γ), there is a fairly sizable hump in $\chi(\vec{q})$ around $|\vec{q}| = 0.7$. This corresponds well with the position of the observed longitudinal-acoustic-phonon anomaly, and a peak in $\chi(\vec{q})$ would be reflected as a dip in $\omega_{LA}(\vec{q})$. However, the magnitude of the hump is too small to presently make a strong connection between it and the anomaly.

Acoustical plasmon-phonon interactions have been proposed[10] as one of the more novel explanations of the phonon anomalies in Nb and other high-T_c superconductors. If present, acoustical plasmons would be reflected by a strong frequency dependence of $\chi(\vec{q}, \omega)$ in the phonon frequency range. In calculations of $\chi'(\vec{q}\omega)$ that we have done at several $\vec{q}$ points, the frequency dependence of the susceptibility is negligible, amounting to only a percent or two from $\omega = 0$ to $\omega = 10$ meV, and the resonance condition $\mathrm{Re}\epsilon(\vec{q}, \omega) = 0$ is far from being satisfied. However, acoustical plasmons should be quite sensitive to the details of the band structure and the Fermi surface. They might also be masked by our approximation of the Fermi factors as having magnitude zero or one throughout the small cubes as determined from their values at the center of the cube.

IV. CONCLUSION

We have calculated the static electronic susceptibility of niobium along the [100] direction by using fitted Slater-Koster energy bands, both with approximate band and momentum-dependent matrix elements and with all matrix elements set equal to one. The results show first the need to carry the numerical integrations far enough toward convergence to rule out spurious structure. This unfortunately requires rather generous amounts of computer time. Because the Gaunt factors are largest for the $l = l'$ and $L = 0$ contributions to the matrix elements in Eq. (5), inclusion of matrix elements causes a form-factorlike reduction in $\chi(\vec{q})$ as $\vec{q}$ increases. We have also found that including the band and momentum dependence of the matrix elements introduces structure which is masked in the constant-matrix-element calculation. This effect is opposite to that found by Gupta and Sinha[16] in their chromium calculation, where including matrix elements decreased structure which was present in the constant-matrix-element calculation. Our results are also quite different from those obtained by Evenson *et al.*[14] for niobium. They found structure in the constant-matrix-element calculation and speculated that part of it would be reduced when matrix elements are included. We suspect that this structure was generated primarily by their numerical-integration scheme.

The susceptibility curve along the [100] direction does exhibit a small hump at about the same $\vec{q}$ value as the [100] LA-phonon anomaly but more work is needed to definitely establish its connection with the phonon spectrum. Work is now in progress on extending the present calculations to include off-diagonal terms of the susceptibility and to integrate them into an electronic screening calculation of the phonon dispersion curves.

ACKNOWLEDGMENTS

The authors are grateful to R. F. Wood and H. G. Smith for providing much of the stimulus to work on this problem, and to F. M. Mueller for helpful conversations.

---

*Research sponsored by the U.S. Atomic Energy Commission under contract with Union Carbide Corp.

[1]S. H. Liu, R. P. Gupta, and S. K. Sinha, Phys. Rev. B 4, 1100 (1971).

[2]J. F. Cooke and H. L. Davis, AIP Conf. Proc. 10, 1218 (1973).

[3]R. D. Lowde and C. G. Windsor, Adv. Phys. 19, 813 (1970).

[4]E. D. Thompson, Phys. Rev. Lett. 19, 635 (1967).

[5]Y. Nakagawa and A. D. B. Woods, Phys. Rev. Lett. 11, 271 (1963).

[6]R. I. Sharp, J. Phys. C 2, 421 (1969); J. Phys. C 2, 432 (1969).

[7]H. G. Smith and W. Gläser, in *Proceedings of the International Conference on Phonons, Rennes, France, July*, 1971, edited by M. Nusimovici (Flammarion, Paris, 1971).

[8]H. G. Smith, Phys. Rev. Lett. 29, 353 (1972).

[9]W. Weber, H. Bilz, and U. Schröder, Phys. Rev. Lett. 28, 600 (1972); W. Weber (unpublished).

[10]B. N. Ganguly and R. F. Wood, Phys. Rev. Lett. 28, 681 (1972).

[11]S. T. Chui, Bull. Am. Phys. Soc. 18, 327 (1973).

[12]S. K. Sinha, in a paper presented at the Symposium on Superconductivity and Lattice Instabilities, Gatlinburg, Tennessee, September 1973 (unpublished).

[13]M. I. Korsunskii, Ya. E. Genkin, V. I. Markovnin, V. G. Zavodinskii, and V. V. Statsuk, Fiz. Tverd. Tela 13, 2138 (1971)[Sov. Phys.-Solid State 13, 1793 (1972)].

[14]W. E. Evenson, G. S. Fleming, and S. H. Liu, Phys. Rev. 178, 930 (1969).

[15]L. F. Mattheiss, Phys. Rev. 139, A1893 (1965).

[16]R. P. Gupta and S. K. Sinha, Phys. Rev. B 3, 2401

(1971).
[17]H. Ehrenreich and M. H. Cohen, Phys. Rev. 115, 786 (1959).
[18]David Pines, *Elementary Excitations in Solids* (Benjamin, New York, 1963), Chap. 4, p. 168.
[19]J. C. Slater and G. F. Koster, Phys. Rev. 94, 1498 (1954).
[20]J. W. D. Connally, in *Electronic Density of States*, edited by L. H. Bennett, Natl. Bur. Stds. Spec. Publ. No. 323 (U.S. GPO, Washington, D.C., 1971).
[21]J. F. Cooke and R. F. Wood, Phys. Rev. B 5, 1276 (1972).
[22]G. Gilat and L. J. Raubenheimer, Phys. Rev. 144, 390 (1966).
[23]F. M. Mueller, J. W. Garland, M. H. Cohen, and K. H. Bennemann, Ann. Phys. (N.Y.) 67, 19 (1971).
[24]J. Korringa, Physica (Utr.) 13, 392 (1947).
[25]W. Kohn and N. Rostoker, Phys. Rev. 94, 111 (1954).
[26]R. A. Deegan and W. D. Twose, Phys. Rev. 164, 993 (1967).
[27]It is interesting that the niobium band structure seems to be harder to fit with the Slater-Koster interpolation scheme than other bcc transition metals. For example, we have reproduced Connally's (Ref. 20) quoted rms deviations of 0.003 and 0.001 Ry. for Fe and Cr, but we have not been able to do better than 0.007 Ry. for Deegan and Twose's (Ref. 26) Nb band structure. This however, is still a good fit for our purposes.
[28]L. F. Mattheiss, Phys. Rev. B 1, 373 (1970).